Color effects in a near-threshold Schmitt trigger

F. Marchesoni
Dipartimento di Fisica, Università di Camerino,
and Istituto Nazionale di Fisica della Materia, I-62032 Camerino, Italy

F. Apostolico, L. Gammaitoni, and S. Santucci
Dipartimento di Fisica, Università di Perugia
and Istituto Nazionale di Fisica della Materia, I-06100 Perugia, Italy
(Received 7 April 1998; revised manuscript received 21 July 1998)

A symmetric Schmitt trigger pumped by both a colored noise and a periodic signal is investigated in the near-threshold regime, where the amplitude of the periodic signal is set slightly above the trigger threshold. The trigger performances are shown, both theoretically and numerically, to be extremely sensitive to increasing the noise correlation time. Noise-induced resonances are analyzed in some detail. [S1063-651X(98)07612-0]

PACS number(s): 05.40.+j, 85.30.De

I. INTRODUCTION

A symmetric Schmitt trigger (ST) is a well-known electronic device [1] characterized by a two-state output and a hysteretic loop (Fig. 1). The trigger output rests in state—as long as the input voltage $V(t)$ is smaller than a threshold value V_0. As $V(t)=V_0$ the trigger switches (almost) instantaneously into the + state and sits there as long as $V(t)>-V_0$. Typically, the ST input is made up of two components, whose amplitudes greatly depend on the experimental circumstances, namely: (i) a noisy signal with zero mean and finite correlation time; (ii) one or more embedded periodic signals with arbitrary wave forms. In the following we consider input signals $x(t)$ of the form

$$x(t)=\xi(t)+f(t), \tag{1.1}$$

where $f(t)$ is a modulation with period $T_\Omega=2\pi/\Omega$ and $\xi(t)$ is a Gaussian stationary noise with average $\langle\xi(t)\rangle=0$ and autocorrelation function

$$\langle\xi(t)\xi(0)\rangle=\sigma^2 e^{-|t|/\tau}. \tag{1.2}$$

Here, the $\xi(t)$ standard deviation σ is termed noise intensity and the quantity $D=\sigma^2\tau$, the noise strength. The most common choice for the periodic function $f(t)$ is the sinusoidal wave form

$$f(t)=A_0\cos(\Omega t+\phi), \tag{1.3}$$

where ϕ is any initial phase. A symmetric square wave form with amplitude A_0 and period T_Ω provides an even simpler example of the modulation signal $f(t)$. The amplitude A_0 is to be tuned with respect to the *fixed* trigger thresholds $\pm b$ (with $b\geq 0$). With regard to the relevant time scales, we assume Ω to be constant, while the noise correlation time τ may be varied at one's convenience over the whole range $(0,\infty)$. The ST output $y(t)$ is a symmetric dichotomic signal with values $\pm y_m$, chosen arbitrarily. Of course, the modulation $f(t)$ in the input signal (1.1) drives a periodic component $\langle y(t)\rangle$ in the output with the same period T_Ω.

We discriminate between two operating ST configurations: (a) The *subthreshold* regime $A_0<b$. Under such a condition *stochastic resonance* (SR) is clearly observable [2]; the amplitude $\overline{y}(\sigma)$ of the output harmonic component with angular frequency Ω shoots up with increasing noise intensity σ until it reaches a maximum at $\sigma=\sigma_{\rm SR}$ and then dies away for larger σ values [3–5]. Stochastic resonance in a ST is by now a well-established phenomenon [6]. (b) The *suprathreshold* regime $A_0>b$. In this configuration the trigger switches are tightly driven by the input modulation $f(t)$; random failure events may occur due to the noise input component $\xi(t)$. A similar occurrence was predicted recently for a wide class of continuous bistable systems; its evidence is

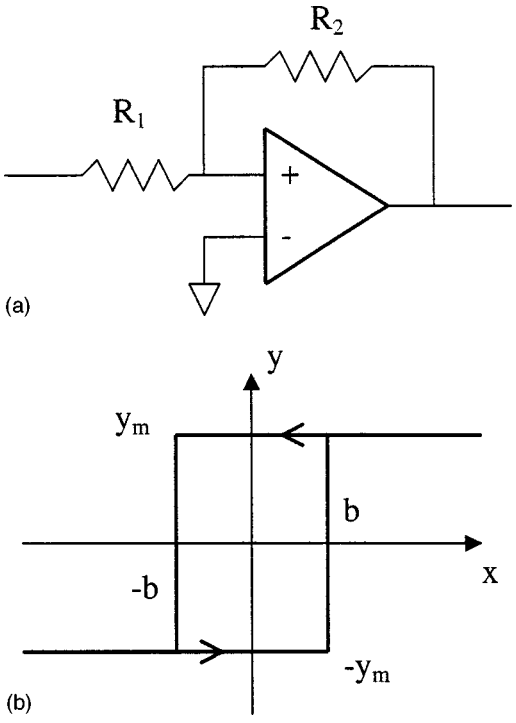

FIG. 1. (a) Circuit diagram of the ST. The threshold b is determined by the ratio R_1/R_2; (b) ST characteristic curve in the notation of Eq. (1.1).

maximum for a certain value of the noise strength and the term *resonant trapping* was coined [7]. A closely related mechanism has been detected in the transient response of certain metastable devices, as well, and goes under the name of noise-enhanced stability [8]. Finally, we recall that the ST is just one particular (though very popular) case of threshold device [9]; therefore, most of the results presented here are of wide applicability to the design and testing of switch devices.

II. THE SUBTHRESHOLD REGIME

Assuming that the switching time is negligible compared to all other circuit time scales, which is often the case, the symmetric ST can be safely regarded as a *bistable threshold* device. In the limit of *weak* forcing $A_0 \ll b$ the switch statistics is governed by one characteristic time $T_0(b)$ that, as prescribed by the linear response theory, is independent of the forcing amplitude A_0. At low noise a good choice for $T_0(b)$ is represented by the mean first-passage time (MFPT) for $\xi(t)$ to diffuse from, say, the lower $-b$ to the upper threshold $+b$. Indeed, under the additional condition that the trigger has switched state at $\xi=-b$, this MFPT reproduces well the mean residence time of the ST in the $-$ state. Of course, changing $\pm$ with $\mp$ does not affect our estimates of $T_0(b)$. Simple algebraic manipulations [10,11] yield

$$T_0(b)=2\sqrt{\pi}\tau\int_0^{\bar{b}} e^{y^2}dy \simeq \tau\sqrt{2\pi}(\sigma/b)e^{b^2/2\sigma^2}, \quad (2.1)$$

with $\bar{b}=b/\sqrt{2\sigma^2}$. The approximate equality holds in the weak noise limit $\bar{b}\gg 1$ [6]. The opposite limit leads to $T_0(b)\sim 1/\sigma$, but threshold crossings and trigger switches are not in as close coincidence as at low noise; hence the MFPT from $-b$ to $+b$ and the switch time may differ [12].

An alternate estimate of the switch time $T_0(b)$ can be obtained as follows. We first imagine recording the input and output signal at time t_0; for instance, $\xi(t_0)=\xi_0$ and $y(t_0)=-y_m$. Then we compute $T_0(b,\xi_0)$, the MFPT for $\xi(t)$ to diffuse from the starting point ξ_0 up to the threshold $+b$. Note that here no trigger switch is assumed at t_0 [12]. Repeating this procedure amounts to an additional average of $T_0(b,\xi_0)$ with respect to ξ_0 in the $-$ state interval $(-\infty,b)$. The outcome of such a calculation is a switch time,

$$T_0(b)=\frac{\tau\sqrt{\pi}}{1+\Phi(\bar{b})}\int_{-\infty}^{\bar{b}} e^{x^2}[1+\Phi(x)]^2dx, \quad (2.2)$$

with $\Phi(x)=(2/\sqrt{\pi})\int_0^x e^{-z^2}dz$, which coincides with the prediction of Eq. (2.1) for $\bar{b}\gg 1$ and approaches $T_0(b)=\tau\ln 2$ for $\bar{b}\ll 1$. [For details see Sec. III A.]

At low forcing frequencies SR occurs experimentally for small to intermediate values of the noise intensity [2]. Under such restrictions the amplitude $\overline{y}(\sigma)$ of the fundamental periodic component of the ST output can easily be computed in the two-state model approximation of Ref. [4]. In the present case, the weak periodic forcing (1.3) can be viewed as just a time modulation of the thresholds, namely $\pm b\to b_\pm(t)\equiv \pm b\mp A_0\cos(\Omega t+\phi)$. On substituting $\pm b$ with $b_\pm(t)$ in Eq. (2.1), we recover the same type of time modulated rates, which are postulated in Ref. [4] (see the Appendix). A straightforward calculation for the asymptotic output autocorrelation function $\langle y(t)y(t')\rangle_{as}=\langle y^2(\sigma)\rangle\cos[\Omega(t-t')]$ yields

$$\langle y^2(\sigma)\rangle=(1/2)\overline{y^2}(\sigma)=\frac{y_m^2}{2}\left(\frac{A_0 b}{\sigma^2}\right)^2\frac{\mu_1^2(b)}{\Omega^2+\mu_0^2(b)}, \quad (2.3)$$

where $\mu_1(b)=\partial\mu_0(\bar{b})/\partial\bar{b}^2$ and $\mu_0=2/T_0(b)$. We remark that Eq. (2.3), as shown in the more general context of the theory of susceptibility, applies to the (linear) response of any low-noise symmetric bistable system [13].

The numerical simulation results for a subthreshold ST are displayed in Fig. 2. The simulation outcome and the two-state model predictions could not be reconciled any better,

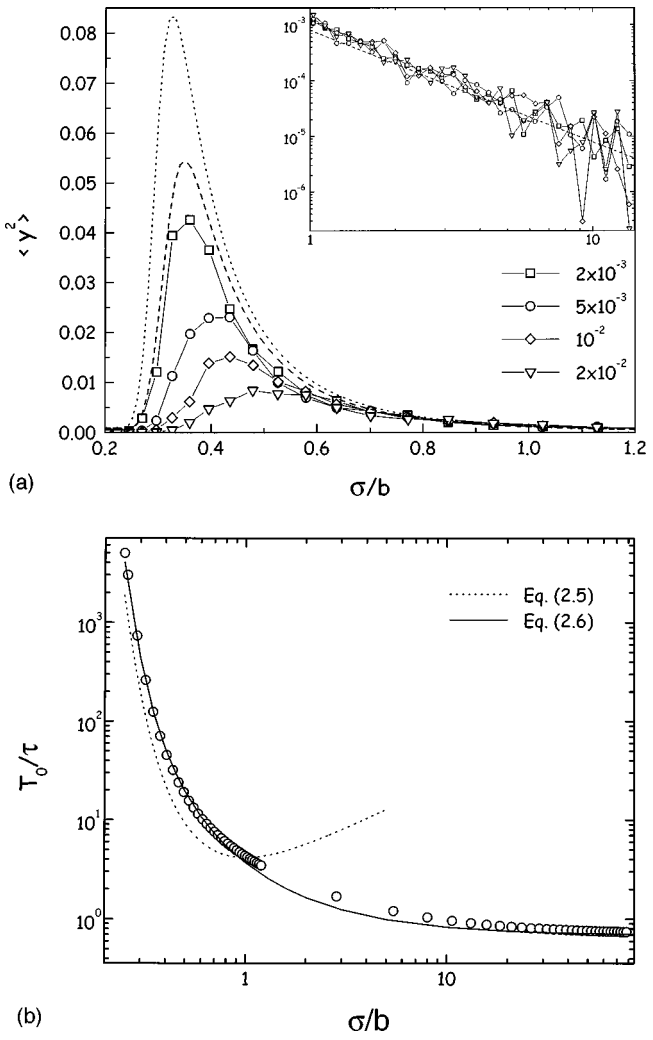

FIG. 2. (a) Subthreshold regime: $\langle y^2(\sigma)\rangle$ (in units of y_m^2) versus σ/b for different values of τ/T_Ω. The input-output parameters and σ are expressed in dimensionless units, i.e., $A_0=10$ and $b=200$. The approximate curve (2.3) is drawn for the smallest $\Omega\tau$ value with $T_0(b)$ given in Eq. (2.2) (dotted line). Inset: decay of $\langle y^2(\sigma)\rangle$ for $\sigma\gg b$ and the strong noise limit of Eq. (3.13) for a sinusoidal modulation (dashed line). The strong noise limit $\sigma\gg b$ is discussed at the end of Sec. III A. (b) The time constant $T_0(b)$ versus σ/b in the absence of periodic forcing. The simulation outcome for two values of the integration time step δt is compared with the predictions of Eqs. (2.1) (dotted line) and (2.2) (solid line).

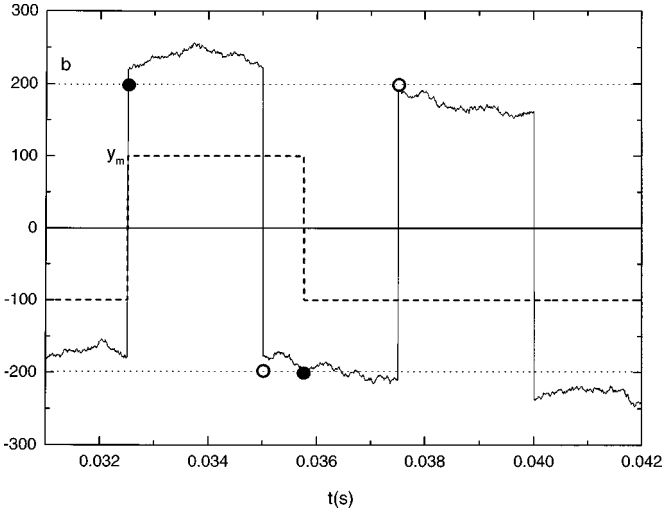

FIG. 3. Input-output scheme (solid and dashed lines, respectively) for a suprathreshold ST driven by a square wave with amplitude $A_0=201$ and frequency $\nu_\Omega=\Omega/2\pi=100$ Hz. Thick dots denote a switch event; empty dots denote a failure.

not even at smaller forcing amplitudes; note that in Fig. 2(a) we set $A_0/b=0.05$, consistently with the linear response requirement $A_0/b\ll(\sigma/b)^2$. In Fig. 2(b) the numerical results for $T_0(b)$ are contrasted with the small noise approximation (2.1) and our prediction (2.2).

III. THE SUPRATHRESHOLD REGIME

In this configuration the forcing amplitude A_0 is taken to be larger than the threshold b, so that the switching dynamics is driven by the forcing signal itself. This is certainly true at low noise intensities, i.e., for $\sigma\ll(A_0-b)$. On increasing σ it might happen that, when $f(t)$ crosses the upper (lower) threshold, the noise signal $\xi(t)$ is smaller than $-(A_0-b)$ [larger than (A_0-b)]. In such a case the switch event gets frustrated, unless $\xi(t)$ recrosses the boundary $-(A_0-b)$ [or (A_0-b)] prior to the subsequent sign reversal of $f(t)$. This mechanism, illustrated in Fig. 3 for the simple case of a squarewave with amplitude A_0 and period T_Ω, describes a noise-induced failure in the temporal sequence of the ST switches.

A similar failure mechanism was observed first in a dynamical system, namely, a quartic double-well potential driven by a forcing term with an amplitude larger than its dynamical bistability threshold [7]: There, a frustrated switch is attributable to the fact that the finite escape time out of the unstable well increases with noise at low intensities and is maximum for an optimal value of σ, hence the term *resonant trapping*. A ST is a threshold device and provides no proper trapping condition by itself (no potential well is involved); however, the failure mechanism predicted above may be viewed as the natural counterpart of resonant trapping in a continuous bistable system, which takes place for long noise correlation times (*strong color* limit [11]). To investigate such a mechanism we consider the following two cases here:

A. Square-wave signal

This is the case sketched in Fig. 3. The condition for a *failure event* can be stated as follows.

(a) At the time $t=0$, when the forcing signal changes sign, say, from $-A_0$ to A_0, we require that $\xi(0+)<-(A_0-b)$. This condition occurs with probability

$$P[\xi<-(A_0-b)]=\int_{-\infty}^{-(A_0-b)}p(\xi)d\xi$$

$$=(1/2)P[|\xi|>(A_0-b)]. \qquad (3.1)$$

The noise $\xi(t)$ is not allowed to recross the boundary $-(A_0-b)$ for a whole half forcing period, i.e., for $t\leqslant T_\Omega/2$, lest a switch event occurs anyway, though with time delay. The failure probability decays exponentially with T_Ω, the relevant time constant $T_1(b)$ being the average recrossing time from $\xi(0)$, with $\xi(0)<-(A_0-b)$ to $-(A_0-b)$.

Now we calculate the recrossing time constant $T_1(b)$ in a symmetric ST. Let us assume that at $t=0$ the noise $\xi(t)$ satisfies condition (a), that is, $\xi(0)\equiv\xi_0<-(A_0-b)$. The MFPT for $\xi(t)$ to diffuse from ξ_0 up to the absorbing boundary $-(A_0-b)$ (with $\xi=-\infty$, a reflecting barrier) is [10]

$$T_1(b,\xi_0)=\frac{\tau^2}{D}\int_{\xi_0}^{-(A_0-b)}\frac{dy}{p(y)}\int_{-\infty}^{y}p(x)dx. \qquad (3.2)$$

On introducing the definition of error function $\Phi(x)=(2/\sqrt{\pi})\int_0^x e^{-z^2}dz$, we obtain

$$T_1(b,\xi_0)=\tau\sqrt{\pi}\int_{\bar{\xi}_0}^{-(\bar{A}_0-\bar{b})}e^{x^2}[1+\Phi(x)]dx, \qquad (3.3)$$

with $\bar{\xi}_0=\xi_0/\sqrt{2\sigma^2}$ and $\bar{A}_0=A_0/\sqrt{2\sigma^2}$. Finally, we take the average of $T_1(b,\xi_0)$ over ξ_0 in the allowed range $(-\infty, -(A_0-b)]$, i.e.,

$$T_1(b)=\int_{-\infty}^{-(A_0-b)}p(\xi_0)T_{1-}(b,\xi_0)d\xi_0/\int_{-\infty}^{-(A_0-b)}p(\xi_0)d\xi_0. \qquad (3.4)$$

The double integral of Eq. (3.4) can be approximated analytically in two limits: for $\bar{A}_0-\bar{b}\gg1$ (small noise),

$$T_1(b)=\tau[\sigma/(A_0-b)]^2, \qquad (3.5)$$

and for $\bar{A}_0-\bar{b}\ll1$ (strong noise),

$$T_1(b)=\tau[c_1-c_2(A_0-b)/\sigma], \qquad (3.6)$$

with $c_1=\sqrt{\pi}\int_0^\infty e^{x^2}[1-\Phi(x)]^2dx=\ln 2$ and $c_2=\sqrt{\pi}/2-\ln 2/\sqrt{\pi}$.

Combining Eqs. (3.1) and (3.2) gives the probability that a failure takes place, namely

$$(1/2)P[|\xi|>(A_0-b)]\exp[-(1/2)T_\Omega/T_1(b)]. \qquad (3.7)$$

The probability (3.7) vanishes for $\sigma\to0$ and jumps to a horizontal asymptote $(1/2)\exp(-T_\Omega/2\tau)$ in the neighborhood of $\sigma\sim(A_0-b)$. Most importantly, no resonant behavior is predicted.

On the other hand, the trigger input-output *synchronization* requires that a second condition hold true:

(b) At time $t=0$ when $f(t)$ flips sign, say, from $-A_0$ to A_0, a trigger switch takes place only under the additional

restriction $\xi(0-)<(A_0+b)$, that is, with probability $P[-(A_0-b)<\xi(0)<(A_0+b)]$. As a matter of fact, we must exclude situations where in the following half forcing period $\xi(t)$ takes on values more negative than $-(A_0+b)$, lest a spurious (noise-induced) switch occurs opposite in phase to $f(t)$. The time constant of such a mechanism coincides with the MFPT for $\xi(t)$ to diffuse from ξ_0 in the interval $[-(A_0-b),+\infty)$ down to $-(A_0+b)$, namely,

$$T_2(b,\xi_0)=\frac{\tau^2}{D}\int_{-(A_0+b)}^{\xi_0}\frac{dy}{p(y)}\int_y^{\infty}p(x)dx. \tag{3.8}$$

Following the procedure [(3.2)–(3.4)] developed for calculating $T_1(b)$, we take the average of $T_2(b,\xi_0)$ over the starting point $\xi_0=\xi(0)$ and identify two important limits, namely,

$$T_2(b)\simeq\tau\sqrt{2\pi}\left(\frac{\sigma}{A_0+b}\right)\exp\left[\frac{1}{2}\left(\frac{A_0+b}{\sigma}\right)^2\right]\quad(\sigma\ll A_0+b), \tag{3.9}$$

$$T_2(b)\simeq\tau[c_1+c_2A_0/\sigma+c_3b/\sigma]\quad(\sigma\gg A_0+b), \tag{3.10}$$

with $c_3=\sqrt{\pi}/2+\ln 2/\sqrt{\pi}$.

In the strong color limit $\Omega\tau\gg1$, the amplitude $\overline{y}(\sigma)$ of the output periodic component with angular frequency Ω can be computed explicitly within the framework of the two-state model [4]. At variance with the subthreshold case of Sec. II, the transition rates between the $\pm$ states are conditioned by the trigger state at the time when the external modulation $f(t)$ reverses its sign. For instance, let $f(t)$ switch from $-A_0$ to A_0 at time $t=0$. If $y(0)=-y_m$, then $T_1(b)$ coincides with the reciprocal of the transition rate from the $-$ to the $+$ state; analogously, $T_2(b)$ may be taken as the inverse transition rate from the $+$ to the $-$ state. Note that for $\Omega\tau\gg1$ the crossing mechanisms in opposite directions may be taken as statistically unrelated. A simple calculation (see the Appendix) yields the asymptotic output autocorrelation function $\langle y(t)y(t')\rangle_{as}=\langle y^2(\sigma)\rangle\cos[\Omega(t-t')]$, with

$$\langle y^2(\sigma)\rangle=(1/2)\overline{y^2}(\sigma)=\frac{1}{2}\left(\frac{4}{\pi}y_m\right)^2\frac{T_1^{-1}-T_2^{-1}}{\sqrt{(T_1^{-1}+T_2^{-1})^2+\Omega^2}}. \tag{3.11}$$

The factor $4y_m/\pi$ is the Fourier coefficient of the fundamental harmonic component of a periodic square wave with amplitude y_m.

In the *near-threshold* regime $A_0\to b+$, Eq. (3.11) predicts that the curves $\langle y^2(\sigma)\rangle$ versus σ for large noise correlation times drop sharply at $\sigma\sim(A_0-b)$ and $\sigma\sim(A_0+b)$ and flatten out in between, thus forming a plateau. We checked that the quantitative agreement with the numerical simulation displayed in Fig. 4 is quite close. In the plateau region $(A_0-b)\ll\sigma\ll(A_0+b)$,

$$\langle y^2(\sigma)\rangle=\frac{1}{2}\left(\frac{4}{\pi}y_m\right)^2\frac{1}{\sqrt{1+(\Omega T_1)^2}}, \tag{3.12}$$

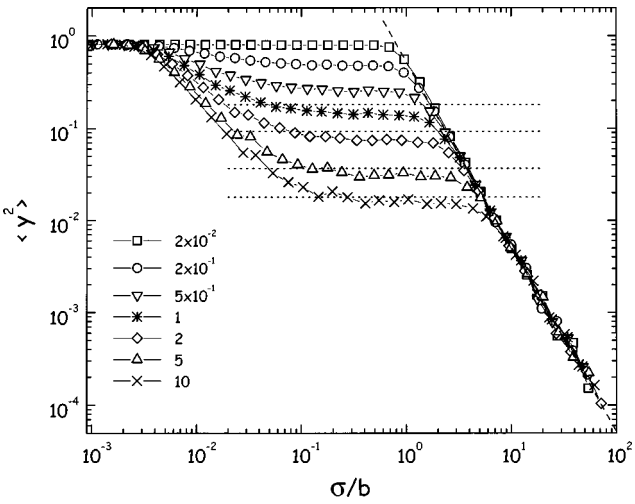

FIG. 4. Suprathreshold regime: $\langle y^2(\sigma)\rangle$ (in units of y_m^2) versus σ/b for a square-wave signal $f(t)$ for several values of τ/T_Ω. The other parameter values, $A_0=201$, $b=200$, and σ are expressed in dimensionless units. Theoretical predictions: the intermediate noise plateau of Eq. (3.12) (dotted lines); the strong noise limit of Eq. (3.13) (dashed line).

with $T_1(b)$ approximated by Eq. (3.6). The first drop of $\overline{y}(\sigma)$ at around $\sigma\sim(A_0-b)$ is due to $T_1(b)$ leveling off to its asymptote $T_1(b)=c_1\tau$ [see Eqs. (3.6) and (3.7)]. The plateau dependence on the dimensionless product $\Omega\tau$ is remarkable: $\langle y^2(\sigma)\rangle=(1/2)\overline{y^2}(\sigma)$ is inversly proportional to $\Omega\tau$ for $\Omega\tau\gg1$. This implies that very few synchronized switches occur in a ST driven by a strongly colored noise with $\sigma\gg(A_0-b)$. *Analog* simulation confirmed this picture of the suprathreshold ST response. In particular, the $\Omega\tau$ dependence of $\langle y^2(\sigma)\rangle$ in the plateau region, Eq. (3.12), proved tenable over three decades, i.e., for $1\leqslant\Omega\tau\leqslant10^3$. This result is rather surprising when compared with the more conventional SR prediction (2.3) for the subthreshold regime.

The second drop of $\overline{y}(\sigma)$ at around $\sigma\sim(A_0+b)$ can be explained by noticing that $T_2(b)$ approaches $T_1(b)$ for $\sigma\gg(A_0+b)$ [see Eqs. (3.6) and (3.10)] and that $\langle y^2(\sigma)\rangle$ is proportional to the difference $T_2(b)-T_1(b)$ [see Eq. (3.11)]. However, the resulting decay law $\langle y^2(\sigma)\rangle\sim1/\sigma$ is at variance with the outcome of our simulations (Figs. 4 and 5), where $\langle y^2(\sigma)\rangle$ falls off apparently like $1/\sigma^2$. Such a discrepancy is amenable to the fact that the two-state model fails for exceedingly large noise intensities $\sigma\ll(A_0+b)$ (see the Appendix). As explained in item (b), the instantaneous switch probability from the $-$ state to the $+$ state is given by $P_s(\sigma)\equiv P[-(A_0-b)<\xi<(A_0+b)]$. For $\sigma\gg(A_0+b)$ the probability $P_s(\sigma)$ may be approximated to $\sqrt{2/\pi}(A_0/\sigma)$. On the other hand, at large noise intensities the trigger switches are no longer controlled by the noise correlation time—note that $T_1(b)\sim T_2(b)$ are vanishingly small—whence $\overline{y}(\sigma)=(4y_m/\pi)P_s$ and

$$\langle y^2(\sigma)\rangle=\frac{1}{2}\left(\frac{4}{\pi}y_m\right)^2P_s^2(\sigma)\sim\frac{1}{\pi}\left(\frac{4}{\pi}y_m\right)^2\left(\frac{A_0}{b}\right)^2\left(\frac{b}{\sigma}\right)^2. \tag{3.13}$$

The strong noise limit (3.13) of the curve $\langle y^2(\sigma)\rangle$ is drawn in both Figs. 4 and 5; since no appreciable dependence on

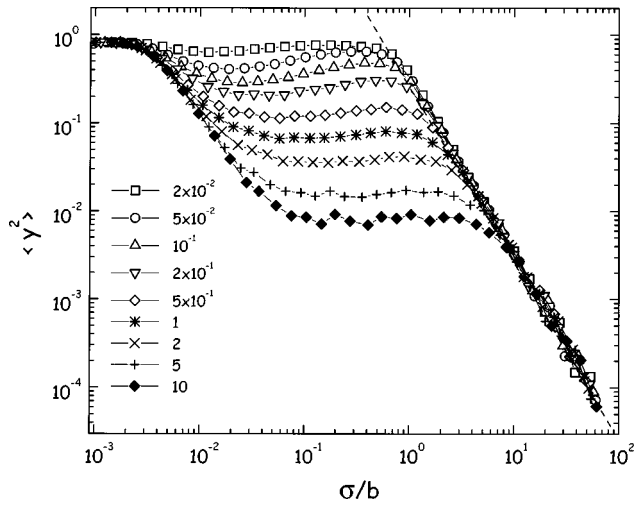

FIG. 5. Suprathreshold regime: $\langle y^2(\sigma)\rangle$ (in units of y_m^2) versus σ/b for the sinusoidal forcing. The values of $\Omega\tau$, A_0, and b are the same as in Fig. 4. The asymptotic curve (3.13), with the substitution $A_0^2 \to A_0^2/2$, is drawn for comparison (dashed line).

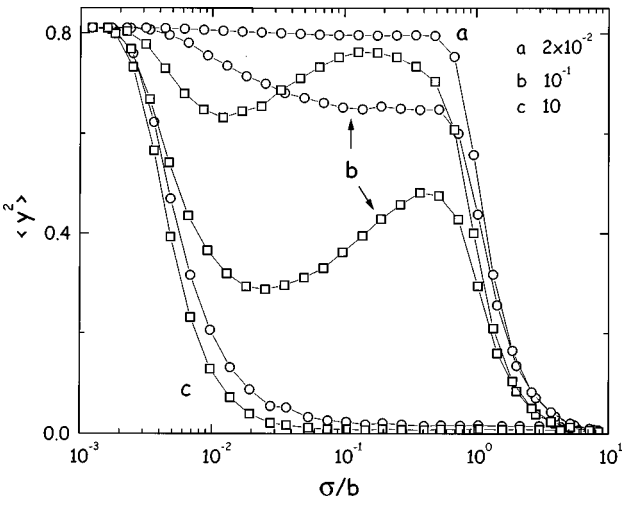

FIG. 6. Suprathreshold regime: $\langle y^2(\sigma)\rangle$ (in units of y_m^2) versus σ/b for different values of τ/T_Ω; the effects of sinusoidal (squares) and square-wave signals $f(t)$ (circles) with the same amplitude and frequency are compared. All other parameter values are the same as in Figs. 4 and 5.

the input parameters τ, Ω and the modulation wave form was detected, one can conclude that such a law is universal. The $\sigma \gg (A_0+b)$ limit for the subthreshold setup of the ST is shown in the inset of Fig. 2(a).

On passing we remark that a similar argument would lead to a simple estimate for $\langle y^2(\sigma)\rangle$ in the ''white noise'' limit $\Omega\tau \to 0$, namely

$$\langle y^2(\sigma)\rangle = \frac{1}{2}\left(\frac{4}{\pi} y_m\right)^2 P^2(|\xi| \geqslant A_0) = \frac{1}{2}\left(\frac{4}{\pi} y_m\right)^2 \Phi\left(\frac{A_0}{\sqrt{2\sigma^2}}\right), \tag{3.14}$$

which is valid throughout the σ domain.

B. Sinusoidal signal

When the ST is pumped by the suprathreshold signal (1.3), the relevant curves $\langle y^2(\sigma)\rangle$ versus σ show a shallow minimum instead of the plateau described in Sec. III A. This is clearly illustrated by the numerical simulation of Fig. 5, where the parameter values A_0, b, τ and Ω are the same as in Fig. 4, the only difference being the $f(t)$ wave form. In Fig. 6 curves from Figs. 4 and 5 are displayed for the sake of comparison. The local maximum of $\langle y^2(\sigma)\rangle$ at $\sigma \sim (A_0 + b)$ bears a certain resemblance to the resonant trapping phenomenon introduced in Ref. [7]; here, however, the reentrant input-output synchronization is sensitive to the continuous wave form of the modulation $f(t)$. Indeed, the overall failure mechanism of Sec. III A could be extended to the present case, though at the price of rather involved algebraic manipulations. It is no surprise that with the same choice of parameter values, $\langle y^2(\sigma)\rangle$ for a sinusoidal modulation $f(t)$ is smaller than for the relevant square wave drive: the corresponding failure probability is larger than our estimate (3.7) because the failure condition (a) must hold now for the time interval $(2/\Omega)\arccos(b/A_0)$, much shorter than $T_\Omega/2$.

The reentrant synchronization mechanism can be qualitatively explained as follows. For $\sigma \ll (A_0 - b)$ a trigger switch occurs only after $f(t)$ has crossed the levels $\pm b$. On raising the noise intensity σ, it may happen that a switch event gets anticipated in time as $f(t)$ approaches $\pm b$ from subthreshold values. Analogously, the failure condition (a) must hold a little longer, since a recrossing could also occur at times when $|f(t)|$ is smaller than but close to b. In other words, the time interval when $f(t)$ acts effectively as a suprathreshold signal increases with the noise intensity. This amounts to lowering the crossing level b by a quantity of the order of σ. As a consequence, $\langle y^2(\sigma)\rangle$ increases slowly with σ within the plateau region $(A_0 - b) \ll \sigma \ll (A_0 + b)$.

This argument can be worked out on more quantitative grounds. The input signal $x(t)$ of Eqs. (1.1)–(1.3) satisfies the stochastic differential equation

$$\dot{x} = -x/\tau + \eta(t)/\tau - (A_0/\tau)\sqrt{1+(\Omega\tau)^2}\sin(\Omega t + \phi - \varphi), \tag{3.15}$$

where $\tan\varphi = (\Omega\tau)^{-1}$ and $\eta(t)$ denotes a zero-mean-valued Gaussian noise with autocorrelation function $\langle \eta(t)\eta(0)\rangle = 2\sigma^2\tau\delta(t)$. At variance with the steady-state approximation of Sec. II, in the strong color regime $\Omega\tau \gg 1$ the intensity of the noise and of the sinusoidal signal becomes comparable for $\sigma/A_0 \sim \sqrt{\Omega\tau}$. Hence, the reentrant synchronization phenomenon in a near-threshold ST must be restricted to noise intensities such that $\sqrt{\Omega\tau} < \sigma/A_0 < 2$, consistently with the results of Fig. 6.

IV. CONCLUSIONS

We have investigated color effects in a symmetric Schmitt trigger pumped by both a time-correlated noise and a periodic signal. Color effects become conspicuous in the near-threshold regime, namely when the amplitude of the periodic signal is set slightly above the trigger threshold. The amplitude of the periodic output component falls off with increasing the noise intensity. For long noise correlation times the trigger output drops first at a noise intensity of the order of the above-threshold component of the periodic signal and, eventually, drops to zero for a noise intensity larger than the

threshold itself. For short correlation times the low-noise output drop is inhibited. In the region in between the trigger output may peak if driven by a continuous wave form (resonant trapping) with forcing period of the order of the noise correlation time. These properties of the trigger response amount to a noise-induced saturation effect, which would take place in a switch device at high forcing frequencies, even under the *ad hoc* assumption of instantaneous switches.

APPENDIX

Our derivation of Eqs. (2.3) and (3.12) follows directly the standard treatment of the two-state model summarized in Ref. [4]. To help the reader rederive our results we now make an explicit connection with McNamara-Wiesenfeld notation [4].

(a) Subthreshold regime. Here we have

$$W_{\pm}(t)=T_0^{-1}[b\pm A_0\cos(\Omega t)], \tag{A1}$$

whence $\alpha_0=1/T_0(b)$. [Note that α_0 is half the switch rate $\mu_0(b)$ of Sec. III A.] Due to the Markovian assumption $\Omega\tau \ll 1$ implicit in Eq. (A1), the rates $W_{\pm}(t)$ depend on the system configuration at time t alone (adiabatic or steady-state approximation).

(b) Suprathreshold regime. As explained in Sec. III A, for $\Omega\tau\gg 1$ our estimates for the suprathreshold transition rates $W_{\pm}(t)$ are *conditioned* by the trigger output $y(t)$ itself. Let $y(t_0)=-y_m$ at $t=t_0$ when $f(t)$ switches from $-A_0$ to A_0; then, in the notation of Ref. [4],

$$W_{+}(t|[-y_m,t_0])=T_2^{-1}(b), \tag{A2}$$

$$W_{-}(t|[-y_m,t_0])=T_1^{-1}(b). \tag{A3}$$

The adiabatic assumption fails for $\Omega T_1(b)\gg 1$ and $\Omega T_2(b)\gg 1$, i.e., for $\sigma\gg(A_0+b)$. The output autocorrelation function $\langle y(t)y(0)\rangle$ must be defined so as to account for the non-Markovian nature of the problem. The appropriate definition in the present case is

$$\langle y(t_1)y(t_0)\rangle=\int dy_0 y_0 p(y_0,t_0)\langle y(t_1)|[y_0,t_0]\rangle, \tag{A4}$$

where $\langle y(t)|[y_0,t_0]\rangle$ is the conditional mean of $y(t)$ given that $y(t_0)=y_0$ for $t_0\leqslant t$. In Eq. (A4) $p(y_0,t_0)=\delta[y_0-y(t_0)]$ and $y(t_0)$ is a square-wave with amplitude y_m and period T_Ω *in phase* with $f(t)$. Following Ref. [4] we now take the limit $t_1,t_0\to\infty$ for $t_1-t_0=t$ fixed. On averaging over the initial phase of the forcing signal $f(t)$, we finally obtain Eq. (3.12).

[1] J. Millman, *Microelectronics* (McGraw-Hill, New York, 1983).

[2] S. Fauve and F. Heslot, Phys. Lett. **97A**, 5 (1983).

[3] L. Gammaitoni, P. Hänggi, P. Jung, and F. Marchesoni, Rev. Mod. Phys. **70**, 223 (1998).

[4] B. McNamara and K. Wiesenfeld, Phys. Rev. A **39**, 4854 (1989).

[5] L. Gammaitoni, F. Marchesoni, E. Menichella-Saetta, and S. Santucci, Phys. Rev. Lett. **62**, 349 (1989).

[6] V. I. Melnikov, Phys. Rev. E **48**, 2481 (1993).

[7] F. Apostolico, L. Gammaitoni, F. Marchesoni, and S. Santucci, Phys. Rev. E **55**, 36 (1997).

[8] M. Gitterman and G. H. Weiss, J. Stat. Phys. **70**, 107 (1993); R. N. Mantegna and B. Spagnolo, Phys. Rev. Lett. **76**, 563 (1993).

[9] Z. Gingl, L. B. Kiss, and F. Moss, Europhys. Lett. **29**, 191 (1995); P. Jung, Phys. Lett. A **207**, 93 (1995).

[10] H. Risken, *The Fokker-Planck Equation* (Springer, Berlin, 1984).

[11] P. Hänggi, P. Jung, and F. Marchesoni, J. Stat. Phys. **54**, 1367 (1989).

[12] The initial threshold crossing $\xi(t_0)=-b$ does not necessarily imply a trigger switch. Indeed, (i) more $-b$ crossings may occur prior to a $+b$ crossing (and the corresponding $-\to+$ switch), hence the switch rate definition $\mu_0=2/T_0(b)$ in Eq. (2.3); (ii) a single $\pm b$ crossing may happen in either direction, whereas a trigger switch requires a definite directionality, that is, $\dot{\xi}(t_0)\gtrless 0$, respectively.

[13] M. I. Dykman *et al.*, Nuovo Cimento D **17**, 661 (1995).